

Journal of Nanophotonics

Nanophotonics.SPIEDigitalLibrary.org

Liquid-phase exfoliation of flaky graphite

Alexandra S. Pavlova
Ekaterina A. Obraztsova
Alexey V. Belkin
Christelle Monat
Pedro Rojo-Romeo
Elena D. Obraztsova

SPIE.

Liquid-phase exfoliation of flaky graphite

Alexandra S. Pavlova,^{a,b,*} Ekaterina A. Obraztsova,^c Alexey V. Belkin,^a
Christelle Monat,^b Pedro Rojo-Romeo,^b and Elena D. Obraztsova^a

^aA.M. Prokhorov General Physics Institute, 38 Vavilova Street, 119991 Moscow, Russia

^bUniversité de Lyon, Lyon Institute of Nanotechnology, Ecole centrale de Lyon,
36, avenue Guy de Collongue, 69131 Ecully, France

^cShemyakin–Ovchinnikov Institute of Bioorganic Chemistry RAS, 16/10,
Miklukho-Maklaya Street, GSP-7, 117997 Moscow, Russia

Abstract. The majority of currently available methods of graphene production have certain drawbacks limiting its scaling. Unlike the others, liquid-phase exfoliation of graphite is a promising technique for high-yield graphene production. In this work, we present our results on one- to four-layer graphene production using various solvents and surfactants from flaky graphite. We suppose that the initial graphite in the form of millimeter-size flakes can be more advantageous for extended graphene flake acquisition than graphite powder consisting of tiny particles used in previous works. Half-centimeter-size graphene films were obtained by depositing exfoliated flakes on an arbitrary substrate. Such films can be useful for electronic and photonic applications. © 2016 Society of Photo-Optical Instrumentation Engineers (SPIE) [DOI: [10.1117/1.JNP.10.012525](https://doi.org/10.1117/1.JNP.10.012525)]

Keywords: graphene; liquid-phase exfoliation; lasers; photonics; Raman spectroscopy.

Paper 15134SS received Oct. 15, 2015; accepted for publication Jan. 15, 2016; published online Feb. 10, 2016.

Currently, graphite appears to be a material attracting the interest of scientists as a basis for graphene production. Graphene is a two-dimensional derivative of graphite and a promising new material, which excels in its outstanding electronic¹ and optical^{2,3} properties. Initially, graphene was obtained by a micromechanical cleavage of graphite.⁴ This technique provides production of very high-quality graphene monolayers, but the output is still extremely low. A promising and cost-effective way to produce graphene is a liquid-phase exfoliation (LPE) technique. LPE of nanotubes (NTs) is a common procedure, allowing separation of individual NTs from the raw powder. It was initially applied for the separation of carbon nanotubes (CNTs).^{5–8} After the first graphene production from graphite (micromechanical cleavage), it was soon proposed that some of the strategies applied for NT exfoliation in liquid-phase could be relevant for graphene and were suggested to be used for graphite powder exfoliation.^{6,7}

The principle of this technique is depicted in Fig. 1 and lies in separating graphite flakes [Fig. 1(a)] by mechanical impact [through applying an ultrasound treatment; Fig. 1(b)] and stabilizing them in a solvent or surfactant solution [Figs. 1(b) and 1(c)]. Finally, centrifugation [CF; Fig. 1(c)] is applied in order to separate thin graphene flakes from the big graphite aggregates. This results in a suspension consisting of thin graphene flakes [Fig. 1(d)].

Such a technique is promising for production of graphene flakes or single carbon NTs in liquid phase with high yield,⁶ low cost,^{9,10} simple scalability, and without expensive growth substrates.¹⁰ Even if the quality of LPE graphene is typically lower¹¹ than that of chemical vapor deposition (CVD) or micromechanical cleaved graphene, it can be useful for many applications, including the mode locking of fiber lasers^{12,13} and photonic crystal fiber lasers.^{14,15} Graphene prepared with the LPE technique can be used in the form of suspensions^{14,15} and can be deposited onto substrates by various methods^{6,9,16–21} or used for free-standing film production.^{6,11–13,21–26} Such composites find wide applications in photonics^{12–15,20,21,26–31} and electronics.^{11,32,33}

*Address all correspondence to: Alexandra S. Pavlova, E-mail: as.pavlova@physics.msu.ru

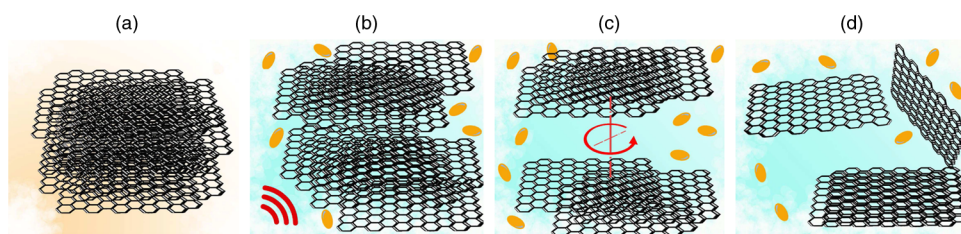


Fig. 1 Schematic of the steps involved in the LPE process: (a) initial bulk graphite; (b) graphite insertion in a solvent or in a surfactant solution (yellow ovals in blue medium) while applying ultrasound (red segments); (c) ultracentrifugation (red circle with arrow) of already separated graphite flakes; (d) resulting thin graphene layers in solution.

Previous studies using the LPE technique were performed for NTs^{7,34} (to obtain single CNTs) as well as for powder graphite^{7,11,22} (in order to obtain graphene flakes). In this work, we used flaky graphite, consisting of 0.5- to 4-mm flat pieces, instead of the commonly used powder graphite (<150 μm). This modification of the initial material should increase the size of output flakes in comparison to graphene obtained from powder graphite.

The result of the LPE technique depends on the medium used for the preparation of graphene suspensions, the ultrasound power, and the CF rates. The choice between solvents and surfactants should be made based on the intended application of graphene. Ultrasonication facilitates exfoliation, and liquid media prevents the aggregation of graphene flakes. Then, ultracentrifugation can be applied to remove unseparated aggregates from the obtained thin graphene suspension. The influence of each LPE process step on graphene is summarized in Table 1 and described in more detail below.

Surfactants adsorb onto the graphite surface of the system and reduce the interfacial free energy,³⁵ decreasing the interaction between carbon derivatives, and by doing so, separating them. The key to better-quality graphite dispersion lies in the Coulomb repulsion between nearby surfactant-coated graphite flakes.⁷ The degree of such repulsion can be quantified via the zeta potential, which was found to increase with decreasing the surfactant size.^{34,36} This allows one to predict that low molecular weight surfactants that pack tightly on the graphite flake surface are ideal for successful exfoliation.^{7,21}

Due to these properties, sodium dodecyl sulphate (SDS) and sodium cholate (SC) appear to be among the most common surfactants used in graphene (and NT) research,^{7,11,23} and were used in the current work.

When a solvent is used for graphene exfoliation, the interfacial (surface) tension between the two should be minimized.^{10,21} For good solvents, one obtains stable dispersions that consist of mono- or few-layer graphene flakes.

The group of Prof. Coleman revealed some guidelines^{6,7} about the exfoliation of carbon NTs in solvents, which apply to graphite exfoliation as well. According to these studies, the best solvents to exfoliate CNTs and graphene possess the same refractive index (about 1.5) and close values of surface energies of graphene/NTs ($\sim 70 \text{ mJ/m}^2$).^{7,9,21} It appears that there are not many suitable solvents,⁷ but *N*-methyl-2-pyrrolidone (NMP) proves to be one of the most appropriate substances for the dispersion of graphene.^{6,10}

Table 1 LPE main steps and their influence on the graphite in solution.

Steps	Influence on graphite	
Liquid media	Surfactant solutions	Adsorb onto the interface, prevent aggregation
	Solvents	Decrease the interfacial tension between solute and solvent
Ultrasonication		Separates graphite into thinner flakes and increases interaction between the flakes and the liquid media
CF		Removes remaining massive aggregates

In general, higher graphene concentrations with better quality (more monolayers in the dispersion) are achieved using surfactants compared to almost all solvents:^{7,10} nearby flakes coated with surfactant will not aggregate due to the Coulomb repulsion.⁷ On the other hand, solvents allow the production of larger flakes,^{7,10} as they experience a higher frictional force (the viscosity is higher than that of water), complicating sedimentation.¹⁰

For the majority of applications (for example, when conductivity is essential, but surfactants are in general insulating⁹), surfactants must be removed after processing,⁷ making solvents more attractive for exfoliation in these situations. On the other hand, the best solvents are toxic and have high boiling points, which in turn complicates their disposal.¹⁰ For biocompatible applications, graphene suspensions are required to be in a water-based solution,³⁷ making surfactants more appropriate for these purposes. The mechanical and optical properties of graphene composites do not suffer from the presence of surfactants, allowing the use of surfactant-based graphene suspensions for, e.g., mode-locking operation. This was demonstrated in a row of groups.^{12,13,21,26,38}

Thus, the choice of proper media for separating graphite flakes falls on the demands of the intended application.

The role of sonication is to separate thick graphite stacks into thinner flakes and thus increase the interaction between graphite flakes and a solvent or surfactant solution. This accelerates further exfoliation of graphene. However, strong sonication can lead to a significant reduction of the graphite flake size. Without sonication, carbon material will be separated as well, but the process will take much longer. Thus, the best solution is to apply a mild ultrasonic power.

Ultracentrifugation is applied to remove the remaining aggregates that were not fully separated after ultrasonication. This improves the dispersion quality in terms of graphene thickness. For NTs, one normally uses CF speeds of about 50,000 revolutions per minute (rpm) and much lower—for graphite powder, about 4000 rpm. After CF, thick and undivided graphite pieces are left at the bottom of a centrifugal tube. The upper part of the solution (~80%) is taken to obtain a dispersion consisting of thin and monolayer graphene flakes. Higher rates of CF will give smaller flakes and decrease the concentration of graphene in the dispersion.

CF helps to remove thick flakes from the dispersion. As an alternative, dilution could do the same work. It was tested on NT dispersion, which was split into two parts:⁷ one part was centrifuged and the other was diluted with the original surfactant to reach the same concentration as the first half after CF. Analysis showed that the ultracentrifuged sample exhibited more individual NTs, but it led to a significant waste of material as well. Thus, the preferred technique depends on the application of the material.

The CF rate is chosen empirically for every combination of solvents and surfactants so that only few layers of graphene are left in the solution, providing a high-quality solution that does not produce any sediment over a period of months.

Previous studies related to the LPE technique were conducted mostly on NTs and graphite powder.

Based on the data for CNT and powder graphite, for the LPE of flaky graphite, we chose two types of solvents—*isopropanol* (IPA) and *NMP* and surfactants—*SDS* and *SC*. This allowed us to have at least four variants of the LPE process. We did not try to use any mixture of these solvents or surfactants. *SDS* and *SC* are the most utilized surfactants in NT research;^{7,39} the *NMP* solvent has a high solvent rate; along with IPA, it is also considered one of the best solvents for graphite exfoliation.^{23,33,40–44}

Most papers point out that mild ultrasonic treatment preserves the lateral size of graphite powder flakes or the length of CNT. Therefore, two types of ultrasound were applied and compared in this work: ultrasonic processor with sonotrode and ultrasonic bath.

Ultracentrifugation was conducted at 5000 rpm for 30 min. Some authors use even lower speeds (down to 500 rpm), and 5000 rpm was chosen as the minimum provided by our CF machine (Optima MAX E).

Ultrasonic bath: To stabilize the dispersion in the experiment with an ultrasonic bath, we used *NMP*, *IPA*, and *SDS*. The *SDS* solution was prepared by mixing 5 mg of precursors in 1 ml of distilled water. Undiluted *NMP* and *IPA* were used. Graphite was taken in the quantity of 3.5 mg/ml and added to 10 ml of corresponding solvent or surfactant solution.

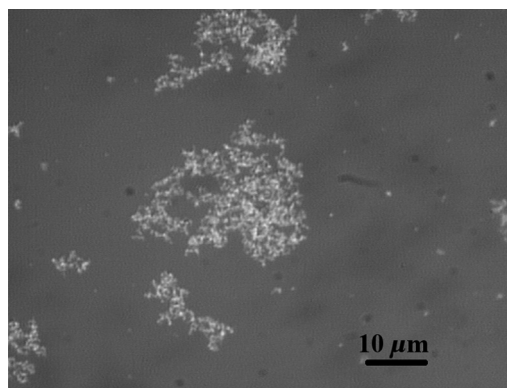


Fig. 2 The optical image of graphene prepared in IPA during 10 h of US bath and deposited on glass.

The graphite solution prepared in IPA (10 h of sonication, ~ 200 W) was drop-casted onto a glass substrate (Fig. 2), with subsequent drying on a hot plate ($\sim 70^\circ\text{C}$). The Raman spectra (514.5-nm excitation wavelength; Fig. 3) showed a 2D peak at about 2700 cm^{-1} . The position, shape, and $I(2\text{D})/I(\text{G}) = 0.28$ ratio conclude that we obtained three- to four-layer graphene.⁴⁵ The optical microscope image and the disorder Raman peaks show that the obtained graphene has a substantial density of defects (intense D peak and appearance of D' peak), which can be caused by the flake edges.

The SDS aqueous solution and NMP were prepared for the investigation of sonication time influence on the quality of graphene suspensions. For this, seven series of experiments were performed with sonication times from 1.5 to 30 h. After each of these periods of time, 3 ml of solution was taken from the main cuvette, the same quantities of NMP or water (in case of SDS) were added to the initial cuvettes, and the ultrasonication was continued. New samples were centrifuged and the upper part ($\sim 70\%$) of solution was decanted for further measurements. The remained sediment was not used. The centrifuged samples were drop-casted onto glass and/or silica substrates, then dried with a hot plate under $\sim 70^\circ\text{C}$. The samples were analyzed by Raman spectroscopy.

All samples sonicated during 1.5 and 3 h showed no graphite peak after ultracentrifugation, indicating a high sedimentation rate due to a poor separation of graphite flakes. However, the absence of Raman peaks can also indicate a low concentration of the material. After 6 h of sonication, only the NMP solution showed graphite characteristics in Raman spectra. It is worth pointing out that all samples produced with SDS and NMP had quite similar Raman

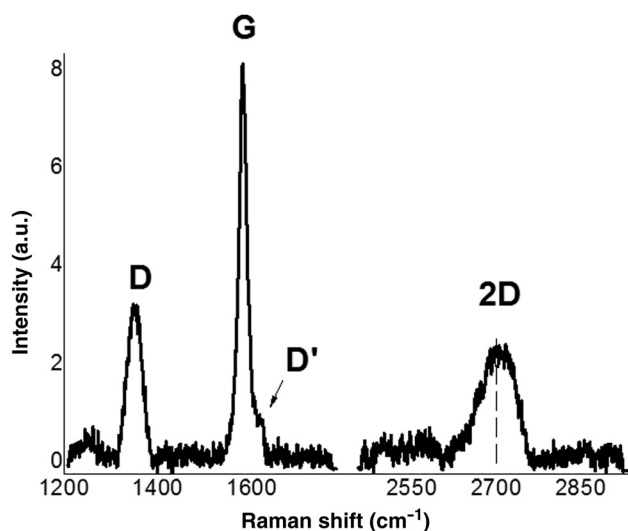


Fig. 3 The Raman spectra ($\lambda_{\text{ex}} = 514.5\text{ nm}$) for graphene prepared in IPA during 10 h of US bath.

characteristics. The SDS and NMP samples sonicated between 9 and 30 h are characterized by spectra, showing $I(2D)/I(G) = 0.22$ and a 2D peak position at about 2704 cm^{-1} (excitation wavelength 514.5 nm) with linewidth of about 75 cm^{-1} (Fig. 4). Taking into consideration the following points, this suggests three- to four-layer graphene formation:

- For one- and two-layer graphene, the 2D peak position is lower than 2700 cm^{-1} on the Raman shift scale (with excitation on 514.5 or 532 nm);^{46–48}
- A five-layered graphene 2D peak can be roughly approximated by two peaks, with a distinguished right part (about 25% higher than the left one; one- to four-layer graphene does not possess such a property);⁴⁵
- Several flakes of monolayer graphene stacked one onto another show lower intensity and higher linewidth ($>24\text{ cm}^{-1}$) of the 2D peak intensity^{47,48} than that of monolayer graphene, as we confirmed in our experiments on CVD-grown graphene.

The defect ratio $I(D)/I(G)$ increased with sonication time. This dependence was monotonous for SDS in a quantitative sense, but for samples prepared with NMP, it was only qualitative. At the same time, it can be seen that NMP gave an almost two times smaller defect ratios than SDS, with the mean values of $I(D)/I(G)$ equaling 0.35 and 0.61 , correspondingly. This can be explained by the higher viscosity of the NMP solution compared with that of the SDS water solution, which results in larger flakes and hence lower D peak signal obtained from the flake edges.^{10,33}

Ultrasonic tip: SDS and SC were used for experiments where ultrasonication was applied to graphene via the sonotrode (tip). Various sonication power values and times were applied.

SDS was used in a concentration of 5 mg/ml (0.5%), and the SC concentration was between 1 and 20 mg/ml (0.1% to 2%). Sonication was applied in a continuous regime for a period of time between 1 and 3 h , with the power varying between 30% and 90% (of maximum 600 W). Drop-casting (as in the previous experiments) and spin-coating were applied to cover the silica substrates with graphene flakes.

Several series of experiments with SDS, where the graphene solution was deposited on a substrate by drop-casting, showed the presence of three- to four-layer graphene (Fig. 5, black curve) with $I(2D)/I(G) = 0.23$, which is about the same value as for the samples obtained using an ultrasonic bath. But some of the samples had more interesting characteristics: values up to $I(2D)/I(G) = 0.4$ with 2D peak linewidth of about 67 cm^{-1} were obtained for the dispersion prepared in SC suspension. For the samples prepared by means of an ultrasonic tip in SC or SDS and deposited onto substrates by drop-casting, the damage ratio $I(D)/I(G)$ was about 0.51 .

For the samples prepared by sonotrode, D peak intensity (the disorder characteristics in samples) was higher, with an average $I(D)/I(G) = 0.82$, compared to that for samples prepared with

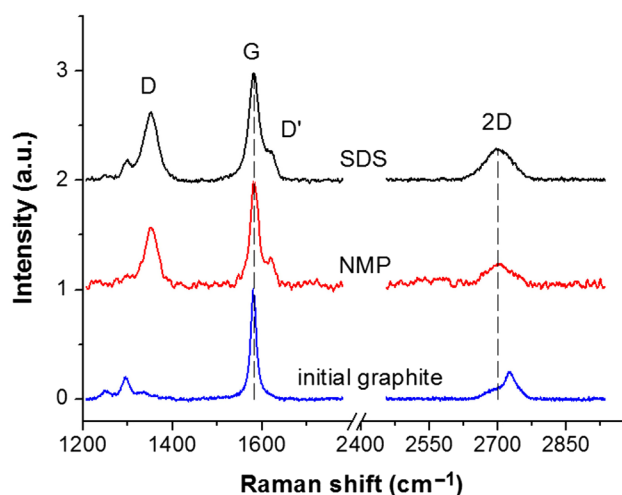


Fig. 4 The Raman spectra for graphene prepared in NMP and SDS after 15 h of US bath. The blue spectrum represents the initial graphite. The vertical dashed line shows 2700 cm^{-1} position.

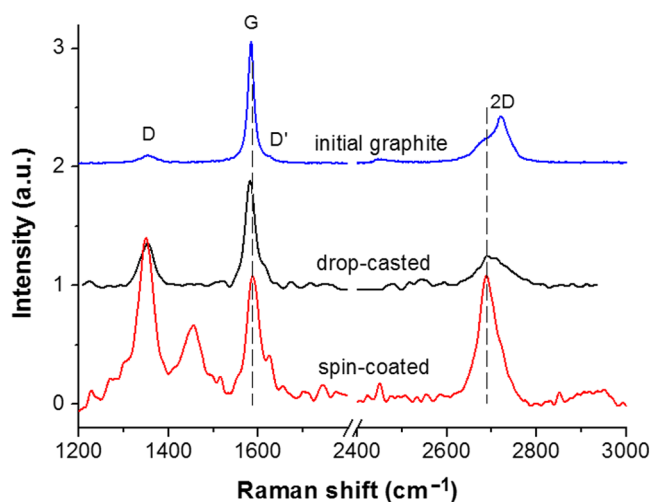


Fig. 5 The Raman spectra ($\lambda_{\text{ex}} = 532 \text{ nm}$) from the initial graphite (blue), drop-casted sample (black; shown in Fig. 6) and spin-coated sample (red), prepared in SC suspension (the residues give the peak on 1450 cm^{-1}).

an ultrasonic bath $I(\text{D})/I(\text{G}) = 0.5$. A tip impact is more aggressive than that of the wide ultrasonic bath.

Along with the Raman (Fig. 5) and optical measurements (Fig. 6), electron microscopy (Fig. 7) was used to investigate the quality of LPE graphene. These experiments were performed on a graphene film obtained via filtration of the suspension through a Millipore cellulose membrane. After filtration, the membrane with the graphene film on it was placed onto a SiO_2/Si substrate, then removed with acetone. Electron microscopy showed the presence of large

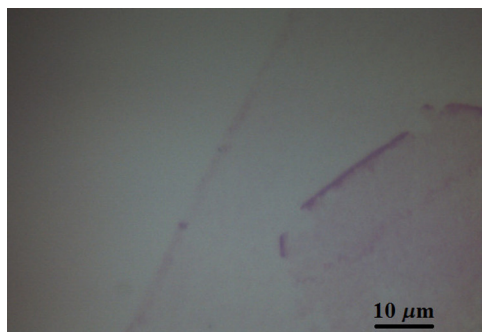


Fig. 6 The optical image of drop-casted graphene flakes (Raman spectra was taken from the center of the image).

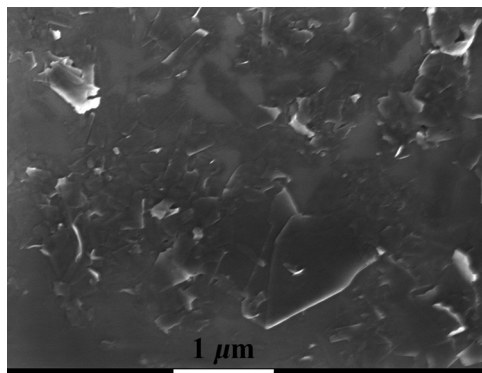


Fig. 7 SEM image of as-fabricated graphene film.

graphene flakes (up to 1 μm in size) along with the smaller flakes (down to 100 nm in size) of higher quantity. This can be observed with an optical and electron microscope.

For further experiments, films of graphene flakes were prepared by the spin-coating technique. The average value of ratio $I(2D)/I(G)$ for samples prepared in this way was about 0.66 and is more than two times higher in comparison with the data obtained for samples produced with the drop-casting method. This conceivably appears due to the effect of the conglomeration of flakes during the drying process after drop-casting. Spin-coating allows a quick distribution of a liquid sample over the substrate surface, takes a very short time (seconds in comparison to minutes needed for drying a drop-casted sample), and leaves less material for conglomeration. It should be mentioned that the size of the flakes left on the substrate after spin-coating can depend on the condition of the process (speed value, for instance). The data obtained from the spin-coated graphene showed a Raman spectrum typical for monolayer graphene (or for a couple of stacked monolayers; Fig. 5, red curve), with $I(2D)/I(G) = 1.1$ and a 2D peak linewidth of 40 cm^{-1} . Even if the material was not clearly observable with the optical microscope, a wider linewidth (40 cm^{-1} instead of 24 cm^{-1}) of the 2D peak and a relatively low value of the 2D and G peak intensity ratio indicated the presence of stacked graphene monolayers. The intensity of the D peak for spin-coated samples was on average about two times higher than for the drop-casted samples, demonstrating a ratio $I(D)/I(G)$ equal to 1.1 and 0.52, correspondingly. This is probably due to the smaller size of flakes that was observed with the optical microscope. The peak at 1450 cm^{-1} appears due to the Raman signal detected from the SC, which was used as the surfactant during the LPE process.

In conclusion, the LPE technique was applied using various media and different methods of ultrasonication and deposition of graphene suspensions. The LPE technique easily provided us with thin graphene layers for all media used for ultrasonication. However, the deposition of the solution onto substrates is a delicate process. Thus, the drop-casting method provided three- to four-layer graphene, while spin-coating showed the presence of monolayer graphene for the solution prepared in the same way. IPA showed a fast sedimentation, in several days, while graphene from other solutions showed no precipitation during several months. The results obtained with NMP and SDS were comparable in terms of graphene thickness. According to the Raman spectra, the NMP-stabilized flakes are characterized by increased lateral dimensions due to the higher solvent viscosity. During the ultrasonic tip experiment, it was revealed that SDS and SC provide the same damage ratio, but SC yields thinner graphene [according to the $I(2D)/I(G)$ ratio value] compared to SDS.

The prepared graphene suspensions were deposited on arbitrary substrates by spin-coating, drop-casting, and filtration. The thinnest films were obtained by the spin-coating technique, while the best uniformity was achieved by transferring the graphene film obtained by filtration through the Milipore filter.

The maximum size of flakes observed in an electronic microscope was about $1.5\text{ }\mu\text{m}$. This value does not exceed the values obtained for powder graphite reported in the literature.^{6,20,41} Lower ultrasonic power and CF rate should provide larger flakes.

In addition to the applications described above, the suspensions obtained by the LPE technique can be deposited gradually onto the substrate in order to cover it several times with carbon material, thus making it more uniform and changing the number of graphene layers. Graphene in the liquid media can be useful for filling the narrow cavities (for instance, in photonic crystal fibers mentioned above), where it could be difficult to input CVD-grown graphene. To avoid graphene stacking in cavities, the suspensions can be filtered to leave only small flakes. Such suspensions allow production of the transparent conductive films useful for electronic or optical applications, such as the formation of touch-screen displays or mode-locking operation, as mentioned earlier.

Acknowledgments

Raman measurements were done in frames of the RSF-15-12-30041 project; graphene flake processing was performed in frames of RFBR projects under Grant Nos. 14-02-31725, 14-02-31498, and 15-32-20941. The support of the French Embassy in Russia and Institut Universitaire de France is also acknowledged.

References

1. A. H. Castro Neto et al., "The electronic properties of graphene," *Rev. Mod. Phys.* **81**(1), 109–162 (2009).
2. R. R. Nair et al., "Fine structure constant defines visual transparency of graphene," *Science* **320**(5881), 1308 (2008).
3. Q. Bao et al., "Atomic-layer graphene as a saturable absorber for ultrafast pulsed lasers," *Adv. Funct. Mater.* **19**(19), 3077–3083 (2009).
4. K. S. Novoselov et al., "Electric field effect in atomically thin carbon films," *Science* **306**(5696), 666–669 (2004).
5. M. J. O'Connell et al., "Reversible water-solubilization of single-walled carbon nanotubes by polymer wrapping," *Chem. Phys. Lett.* **342**(3–4), 265–271 (2001).
6. Y. Hernandez et al., "High-yield production of graphene by liquid-phase exfoliation of graphite," *Nat. Nanotechnol.* **3**(9), 563–568 (2008).
7. J. N. Coleman, "Liquid-phase exfoliation of nanotubes and graphene," *Adv. Funct. Mater.* **19**(23), 3680–3695 (2009).
8. M. F. Islam et al., "High weight fraction surfactant solubilization of single-wall carbon nanotubes in water," *Nano Lett.* **3**(2), 269–273 (2003).
9. X. Han et al., "Scalable, printable, surfactant-free graphene ink directly from graphite," *Nanotechnology* **24**(20), 205304 (2013).
10. F. Bonaccorso et al., "Production and processing of graphene and 2D crystals," *Mater. Today* **15**(12), 564–589 (2012).
11. S. De et al., "Flexible, transparent, conducting films of randomly stacked graphene from surfactant-stabilized, oxide-free graphene dispersions," *Small* **6**(3), 458–464 (2010).
12. Z. Sun et al., "Graphene mode-locked ultrafast laser," *ACS Nano* **4**(2), 803–810 (2010).
13. M. Zhang et al., "Tm-doped fiber laser mode-locked by graphene-polymer composite," *Opt. Express* **20**(22), 25077–25084 (2012).
14. Z. B. Liu, X. He, and D. N. Wang, "Passively mode-locked fiber laser based on a hollow-core photonic crystal fiber filled with few-layered graphene oxide solution," *Opt. Lett.* **36**(16), 3024–3026 (2011).
15. Y. H. Lin et al., "Using graphene nano-particle embedded in photonic crystal fiber for evanescent wave mode-locking of fiber laser," *Opt. Express* **21**(14), 16763–16776 (2013).
16. M. Lotya et al., "Measuring the lateral size of liquid-exfoliated nanosheets with dynamic light scattering," *Nanotechnology* **24**(26), 265703 (2013).
17. I. W. P. Chen et al., "Exfoliation and performance properties of non-oxidized graphene in water," *Sci. Rep.* **4**, 3928 (2014).
18. M. Zhou et al., "Production of graphene by liquid-phase exfoliation of intercalated graphite," *Int. J. Electrochem. Sci.* **9**, 810–820 (2014).
19. A. Ciesielski and P. Samori, "Graphene via sonication assisted liquid-phase exfoliation," *Chem. Soc. Rev.* **43**(1), 381–398 (2014).
20. J. Wang et al., "Broadband nonlinear optical response of graphene dispersions," *Adv. Mater.* **21**(23), 2430–2435 (2009).
21. T. Hasan et al., "Solution-phase exfoliation of graphite for ultrafast photonics," *Phys. Stat. Sol. (b)* **247**(11–12), 2953–2957 (2010).
22. A. A. Green and M. C. Hersam, "Solution phase production of graphene with controlled thickness via density differentiation," *Nano Lett.* **9**(12), 4031–4036 (2009).
23. K. R. Paton et al., "Scalable production of large quantities of defect-free few-layer graphene by shear exfoliation in liquids," *Nat. Mater.* **13**(6), 624–630 (2014).
24. P. May et al., "Approaching the theoretical limit for reinforcing polymers with graphene," *J. Mater. Chem.* **22**(4), 1278–1282 (2012).
25. U. Khan et al., "Development of stiff, strong, yet tough composites by the addition of solvent exfoliated graphene to polyurethane," *Carbon* **48**(14), 4035–4041 (2010).
26. R. Mary et al., "1.5 GHz picosecond pulse generation from a monolithic waveguide laser with a graphene-film saturable output coupler," *Opt. Express* **21**(7), 7943–7950 (2013).
27. A. Martinez et al., "Optical deposition of graphene and carbon nanotubes in a fiber ferrule for passive mode-locked lasing," *Opt. Express* **18**(22), 23054–23061 (2010).

28. L. Zhang et al., "Linearly polarized 1180-nm Raman fiber laser mode locked by graphene," *IEEE Photonics J.* **4**(5), 1809–1815 (2012).
29. B. V. Cuning, C. L. Brown, and D. Kielpinski, "Low-loss flake-graphene saturable absorber mirror for laser mode-locking at sub-200-fs pulse duration," *Appl. Phys. Lett.* **99**(26), 261109 (2011).
30. A. Martinez and S. Yamashita, "10 GHz fundamental mode fiber laser using a graphene saturable absorber," *Appl. Phys. Lett.* **101**(4), 041118 (2012).
31. A. S. Pavlova et al., "Towards an integrated mode-locked microlaser based on two-dimensional photonic crystals and graphene," *J. Nanoelectron. Optoelectron.* **8**(1), 42–45 (2013).
32. G. P. Keeley et al., "Electrochemical ascorbic acid sensor based on DMF-exfoliated graphene," *J. Mater. Chem.* **20**(36), 7864–7869 (2010).
33. F. Torrisi et al., "Inkjet-printed graphene electronics," *ACS Nano* **6**(4), 2992–3006 (2012).
34. Z. Sun et al., "Quantitative evaluation of surfactant-stabilized single-walled carbon nanotubes: dispersion quality and its correlation with zeta potential," *J. Phys. Chem. C* **112**(29), 10692–10699 (2008).
35. M. J. Rosen and J. T. Kunjappu, "Characteristic features of surfactants," in *Surfactants and Interfacial Phenomena*, 4th ed., John Wiley & Sons, Inc., Hoboken, New Jersey (2012).
36. M. Molero et al., "An isotropic model for micellar systems: application to sodium dodecyl sulfate solutions," *Langmuir* **17**(2), 314–322 (2001).
37. Y. Sim et al., "Synthesis of graphene layers using graphite dispersion in aqueous surfactant solutions," *J. Korean Phys. Soc.* **58**, 938–942 (2011).
38. Y. Feng et al., "Saturable absorption behavior of free-standing graphene polymer composite films over broad wavelength and time ranges," *Opt. Express* **23**(1), 559–569 (2015).
39. T. Hasan et al., "Nanotube-polymer composites for ultrafast photonics," *Adv. Mater.* **21**(38–39), 3874–3899 (2009).
40. U. Khan et al., "Solvent-exfoliated graphene at extremely high concentration," *Langmuir* **27**(15), 9077–9082 (2011).
41. U. Khan et al., "High-concentration solvent exfoliation of graphene," *Small* **6**(7), 864–871 (2010).
42. A. O'Neill et al., "Graphene dispersion and exfoliation in low boiling point solvents," *J. Phys. Chem. C* **115**(13), 5422–5428 (2011).
43. F. Bonaccorso and Z. Sun, "Solution processing of graphene, topological insulators and other 2D crystals for ultrafast photonics," *Opt. Mater. Express* **4**(1), 63–78 (2014).
44. J. N. Coleman et al., "Two-dimensional nanosheets produced by liquid exfoliation of layered materials," *Science* **331**(6017), 568–571 (2011).
45. A. Ferrari et al., "Raman spectrum of graphene and graphene layers," *Phys. Rev. Lett.* **97**(18), 187401 (2006).
46. T. A. Nguyen et al., "Excitation energy dependent Raman signatures of ABA- and ABC-stacked few-layer graphene," *Sci. Rep.* **4**, 4630 (2014).
47. L. M. Malard et al., "Raman spectroscopy in graphene," *Phys. Rep.* **473**, 51–87 (2009).
48. A. Ferrari, "Raman spectroscopy of graphene and graphite: disorder, electron-phonon coupling, doping and nonadiabatic effects," *Solid State Commun.* **143**, 47–57 (2007).

Alexandra S. Pavlova graduated in 2011 from the physics department of M.V. Lomonosov Moscow State University, Russia. She is currently working on her thesis in nanophotonics on a co-tutelle agreement between the Institut des Nanotechnologies de Lyon, France, and A.M. Prokhorov General Physics Institute of the RAS, Russia. The research concerns investigation of interaction between photonic crystal microlasers and graphene, in a context of on-chip sources of pulsed laser light.

Ekaterina A. Obratsova obtained her MSc (2005) and PhD (2008) degrees from the physics department of M.V. Lomonosov Moscow State University. Between 2008 and 2009, she worked as a postdoc in the Technical University of Milan. Since 2009, she has worked as a senior researcher in the Electron Microscopy Laboratory of Shemyakin & Ovchinnikov Institute of Bioorganic Chemistry (Moscow, Russia). She is involved in investigation of graphene- and nanotube-like materials by microscopy and optical methods. She is a coauthor of 25 papers.

Alexey V. Belkin graduated from Moscow Technical University of Radioelectronics and Automation in 2012. He received the award for some of the best diploma work. Since September 2012, he has been a PhD student in A.M. Prokhorov General Physics Institute of Russian Academy of Sciences. His activity concerns Raman scattering of different types of nanocarbons. He is a coauthor of four papers.

Christelle Monat worked for 2 years at EPFL, Switzerland, on single-photon sources after obtaining her PhD on integrated microlasers from Ecole Centrale de Lyon, France, in 2003. She joined CUDOS at the University of Sydney in 2005, where she worked on slow light in nonlinear photonic crystals. In 2010, she was appointed an associate professor at Ecole Centrale de Lyon, where she carries out her research on integrated nonlinear optics at INL, France.

Pedro Rojo-Romeo is an associate professor at Ecole Centrale de Lyon (France), and a researcher in the Institute of Nanotechnologies of Lyon (INL). His primary research interests include electrical-optical device fabrication technology and characterization. He works on silicon photonics (functional oxide-based agile optical interconnects), biosensing, energy harvesting, and graphene for photonics and electronics. He has authored/coauthored three patents and 70 publications in international journals, and has 35 participations in invited conferences, and around 100 international conferences.

Elena D. Obraztsova graduated from the physics department of M.V. Lomonosov Moscow State University (MSU) in 1981. She received her PhD in optics at MSU in 1990. Since 1992, she has worked at A.M. Prokhorov General Physics Institute, RAS, heading the Nanomaterials Spectroscopy Laboratory since 2001. Her scientific interests concern optical spectroscopy of low-dimensional materials. She is a coauthor of more than 230 papers in reviewed journals. She was a supervisor of 10 PhD defended theses.